Structural analysis and characterisation technique applied to a CNC vertical machining centre

Ford DG; Widiyarto MHN; Myers A; Longstaff AP; Fletcher S
Centre for Precision Technologies
University of Huddersfield

Abstract

There is a requirement for improved 3D surface characterisation and reduced tool wear, when modern computer numerical controlled (CNC) machine tools are operating at high cutting velocities, spindle speeds and feed-rates. This research project investigates vibration-induced errors on a CNC vertical machining centre under dynamic conditions. A model of the machine structural dynamics is constructed using the Finite Element Method (FEM) for the comprehensive analytical investigation of the machine vibration behaviour. The analytical model is then validated against the measured results obtained from an experimental modal analysis (EMA) investigation. A correlation analysis of the simulated and experimental modal analysis results is undertaken in order to improve the accuracy of the model and minimise modelling practice errors. The resulting optimised model will need further sensitivity analysis utilising parametric structural analysis and characterisation techniques in order to identify a potential for vibration reduction using passive methods.

Keywords

Machine Tool; FEM; EMA; model optimisation; sensitivity analysis

Glossary of Terms:

DDR SDRAM: Dual data rate synchronous dynamic random access memory

GRFP: Global rational fractional polynomial

LDV: Laser doppler vibrometer

MAC: Modal assurance criterion

RFLS: Rational fraction least squares

SDRAM: Synchronous dynamic random access memory

TLM: Transmission line matrix

List of symbols

Small Latin

i: Numerical iteration carried out to find a solution for a small set of base vectors (a subspace)

m: Default dimension of the subspace vectors

n: degrees of freedom or pole pairs

p: Number of eigenvectors requested

p_k: Pole location in the s-plane of the k^{th} mode (eigenvalues)

p_k^*:Conjugate of the k^{th} mode pole

r_k: Complex residue of the k^{th} mode (eigenvectors)

r_k^*: Conjugate of the k^{th} mode complex residue

s: Laplace operator

x(s): Laplace transform of displacement responses

Large Latin

B: System matrix

C : Viscous damping matrix ($N \cdot s \cdot m^{-1}$)

F : Force matrix (N)

F(s) : Laplace transform of applied forces

H: Transfer matrix

$H_k(\omega)$: Transfer function of the k^{th} mode ($m.N^{-1}$)

K: Stiffness matrix ($N \cdot m^{-1}$)

M: Mass matrix (kg)

X; Displacement matrix (m)

Greek

σ_k: Modal damping of the k^{th} mode

μ: Eigenvalue ($rad \cdot s^{-1}$)

ψ: Eigen vector (no unit)

ω: Natural frequency ($rad \cdot s^{-1}$)

ω_k: Modal frequency k^{th} mode

1. Background on machining and process errors

Machine tool vibration is a complex subject requiring a multi-disciplinary approach involving the identification and analysis of the vibration sources and characteristics, as well as its direct and indirect effects. It is influenced and characterised by the machine's structural dynamics, the drive system performance and the cutting force generation. Its effect materialises in the form of poor surface finish of the work-piece, accelerated cutting-tool wear, and chatter during the machining process.

1.1 Machining and machine tool errors

Ford [1] proposed that the design process of any high precision CNC machine tool in order to achieve an ever increasing demand for greater accuracy and therefore a more stringent performance specification must embrace error avoidance,

error measurement, and error compensation techniques. The measurement of the repeatable time and spatial errors can allow compensation methods to be applied to the machine for correction of those errors provided sufficient resolution has been allowed for in the design, with the absolute limit on accuracy for a particular machine being defined by its measured repeatability figures. The main areas of concern affecting component accuracy are environmental effects, user effects and the machine tool static and dynamic accuracy. The sources of error confined to a machine tool are geometrical inaccuracies, thermally induced errors and load errors.

Lui et al [2] emphasised that the control of the machining errors for a milling machine needs the understanding of the process for peripheral milling; and face milling. They illustrated the mechanics of metal cutting for use with multi-tool point operations; provided the knowledge base from previous cutting process modelling; and reported on their investigations into the cutting process dynamics.

Weck [3] related that the vibration types experienced by machine tools are: (a) Free or transient vibrations resulting from impulses transferred to the structure, where the structure is deflected and oscillates in its natural modes of vibration until the damping present in the structure causes the motion to die away. (b) Forced vibrations resulting from periodic forces within the system. The machine will oscillate at the forcing frequency, and if this frequency corresponds to one of its natural frequencies of the structure, the machine will resonate in the corresponding natural mode of vibration. (c) Self excited vibrations resulting from the dynamic instability of the cutting process. This phenomenon is referred to as machine tool chatter, and if large tool- work engagements are attempted, oscillation suddenly builds up in the structure, effectively limiting removal rates.

A book edited by Lopéz de Lacalle and Lamikiz [4] was compiled by a consortium of research specialist together with contributions from industrial partners which dealt with the requirements for future machine tools and their application for high performance machining. It commenced by outlining machine tool basic design principles; the technology history; and current ‘state of the art’ technology. The structure of the machine tool was recognised as a critical issue with the need for new structural component concepts which in turn have a decisive influence on motion accuracy, machine productivity, and machining quality. There should be consideration for parameter eco-efficiency and its decisive influence on the whole life cycle of the machine, especially with the materials and energy resources consumed which was an issue of increasing concern among machine tool builders. It recognised that practices are needed for the optimisation of machine structures, their different configurations, and the need for accurate FEM modelling and for structural passive/active damping.

1.2 Machine process control

Engin and Altinas [5, 6] in their investigations into the mechanics and dynamics of general milling cutters stated that by careful choice of the cutting conditions an optimum metal removal rate (MRR) can be reached to satisfy the need for machine stability. They made available commercial simulation software where chatter avoidance is demonstrated based on the prediction of the stability lobes using the machine conditions with the frequency response function (FRF) of the vibrating structure obtained by modal test [7].

1.3 Machining process modelling

Altinas [8] covered the metal cutting mechanics theory and illustrated the 2-D orthogonal and 3-D oblique cutting processes. He showed that the cutting forces are proportional to the uncut chip area and the specific cutting energy is determined by calibration.

Liu et al [9] proposed a new cutting model with improved dynamic characteristics for peripheral milling with helical end mills. This model was based on the oblique cutting theory and accounted for the chip thickness to enable accurate representation of the cutting forces generated in the machining process. The coefficients used in this investigation were estimated from the cutting trial results performed on a previous investigation. This approach was successfully verified for the peripheral milling processes when the feed rate is higher than the equivalent linear speed of the rotational velocity between adjacent cutting teeth.

Baek et al [10] developed a dynamic model of the surface roughness generated by a face milling process; it considered the static and dynamic components of the cutting process, including the edge profile, cutter run-out, cutting forces and structural vibration. These factors were taken into account to calculate the relative displacement of the work-piece and cutting tool in order to predict the surface roughness. The model was validated by comparison with experimental measurement which illustrated vibration forced vibration marks caused by the cutting process.

Urbikain et al [11] developed a technique for chatter prediction in the straight turning of non-rigid parts, making use of round inserts. They developed an algorithm based a Chebyshev collocation method, which introduced for accurate round insert edge geometry, discretising the lead position angle and the variable cutting coefficients of the forces model along the edge. They claimed the method reached high levels of accuracy since 87.5% of the tested points were successfully predicted.

Moradi et al [12] analysed and produced an extended dynamic model of the milling process, in the presence of internal resonance. Regenerative chatter, structural nonlinearity, tool wear and process damping effects are included in the proposed model. They concluded that machine process parameter optimisation and higher design structural stiffness were necessary for improved performance.

1.4 Machine tool feed drive modelling and system identification

Pislaru et al [13] stated that the modelling used for designing high performance CNC machine tool feed drives should accurately represent the system consisting of three cascaded closed loops for acceleration, velocity and position control. It utilised a modular approach and a hybrid modelling technique which included for distributed load, explicit damping coefficients, backlash and friction. It was used to describe the response of the system under various conditions, and it included for accurate dynamic parameter identification as well as non-linear behaviour effects of the system.

2. Introduction to structural dynamics

2.1 Structural dynamic properties

Altinas [8] outlined that the machine vibration characteristics are dependent on its machine tool elements; the damping of the structural materials used; and its ability to isolate external vibrations that could affect the cutting process and the work-piece quality. An essential analytical tool therefore is the study of the machine tool structural dynamic characteristics through modelling and experimentation.

Modal analysis is one of the tools a designer uses to analyse new product design that involves FEM and EMA. NAFEMS Ltd [14] is globally recognised and the organisation exists to promote the safe and reliable use of Finite Element (FE) and related technology with advice on method /benchmark standards.

Baguley and Hose [15] reviewed and concluded that FEM is used to solve stress analysis, dynamic response, and heat transfer problems; they contain library packages of elements which permit different geometries to be modelled including four, five or six faces which may be flat or curved; the blocks can be distorted into any shape, permitting accurate representations of complex geometric shapes; the shapes of the elements are defined by its 'node' points, which usually lie at the corners or on the edges of the elements; the stiffness of brick elements are calculated by numerical integration, based on assumptions how the element deforms under loads at the node points; providing the elements are sufficiently small.

Schewchuk [16]showed that various algorithms are also available to perform the meshing process, (i.e. the division of a structure into a finite number of smaller elements with individual mass, stiffness, and other relevant properties), such as Delaunay triangulation, paving and mapped methods. The generated elements are checked for conformity to certain requirements (aspect ratio, minimum and maximum angle, etc.) in order to produce robust and accurate solutions. He explained the mathematical connections between mesh geometry, interpolation errors, discretization errors, and stiffness matrix conditioning.

FEM is employed for modelling the structural dynamic properties and several specialised software packages such as ABAQUS, ANSYS, FEMLAB, Nastran, etc. are commercially available. Inter-operability with solid modelling

software (e.g. AutoCAD, CATIA, Pro/ENGINEER, SolidWorks, etc.) has also improved, thus increasing the FEM analysis flexibility and its accuracy. Advancement of computing hardware/software technologies and FEM software to exploit the instruction sets allows faster analysis of more complex and accurate models.

2.2 Experimental modal analysis

The analytical results from structural dynamic models are normally validated using the EMA technique. The dynamic forces introduced to the machine structure are applied via electro-mechanical shakers or instrumented hammers. The dynamic response is then measured by piezoelectric accelerometers as shown by Widiyarto et al [17] or laser Doppler vibrometers (LDV) as shown by Stanbridge and Ewins [18] and converted into FRF data. A dynamic signal analyser is employed to control the disturbance forces, measure the dynamic response of the structure, and process the experimental data. Schwarz and Richardson [19] covered experimental modal analysis theory including the single degree of freedom (SDOF) or multi-degree of freedom (MDOF) curve-fitting algorithms that are employed to extract the structural modal parameters from the measured data. Ewins [20] and Døssing [21] demonstrated that multiple data from one or more experiments using single input multi-output (SIMO) or multi-input multi-output (MIMO) techniques can be analysed simultaneously using global curve fitting methods in order to produce accurate modal parameter estimations.

To achieve accurate experimental modal parameters, comprehensive knowledge of the appropriate equipment selection, experimental configurations and signal conditioning is required. The measurement devices must be able to prevent signal aliasing and leakage as well as yield high signal to noise ratio (SNR) and frequency resolution. The excitation location selection used in the experimental setup influences the frequency bandwidth significantly. In addition, heavy excitation devices can alter the measured results considerably as described in section 3.2 when comparing suspended and worktable mounted shaker configurations.

Note: Impact testing using instrument hammers can be applied in the same way with the added convenience of avoiding a very heavy shaker. However, the high stiffness and damping characteristics of machine tool structures often result in relatively low coherence, a data quality discussed in section 3.2.3, especially around the larger column and bed elements. Varying the hardness of the hammer tip with multiple impacts targeting narrow frequency ranges can help mitigate this but at the expense of reduced efficiency compared to broadband excitation using the shaker.

3.0 Structural investigation of a CNC vertical machining centre

3.1 Machine

Figure 1 show the 3- axis vertical machining centre where the unidirectional Z-axis maximum tool travel is 560mm, and the bidirectional machining table X-axis maximum travel and Y-axis maximum travel are both 510mm. The Siemens 840D CNC controls all the machine tool functions. The spindle speed can be controlled from 60RPM to 8000RPM and

the maximum axis feed-rates are 12m/min (fast traverse 30m/min). The machine utilises Siemens 611 electrical feed drives with permanent magnet synchronous motors (Types 1FK6063 on X-and Y-axis and Type 1FT6064 on Z-axis). The motors for each axis are directly coupling to a ball-screw supported by bearings at both ends and utilise linear bearing guide-ways. The Siemens spindle drive unit provides four quadrant operations through a separately excited Siemens DC motor providing a constant torque range 60RPM to 1500RPM and above 1500RPM constant power range (9KW) to the maximum speed of 8000RPM.

3.2 Experimental modal analysis

3.2.1 Experimental equipment

Medium- and heavy-weight TIRAvib [22] and Brüel & Kjær [23] electro-mechanical shakers are employed to provide the excitation input force to the machine structure. Both devices are employed for the suspended shaker configuration, whereas only the TIRAvib shaker is utilised when the shaker is placed on the worktable due to the workspace restriction.

The excitation force from the shakers is measured by a PCB 221B02 ICP piezoelectric transducer [24] placed between a Modalshop stinger [25] and the driving point located at the machine structure. The structural response data acquisition was measured using either PCB uni-axial industrial grade accelerometers type IMI ICP model 629A11; PCB light weight accelerometers type ICP 353B03; or industrial tri-axial accelerometers type IMI ICP model 623C21which are moved from one set of points to another to obtain the complete measurement data.

The excitation/response transducer signals were captured by a Data Physics SignalCalc Mobilyzer dynamic signal analyser [26]. The signal conditioning was performed automatically via the host computer software using a high-speed network linked to the analyser interface. The signal analyser also generates the shaker low-voltage excitation signal before suitable amplification is applied.

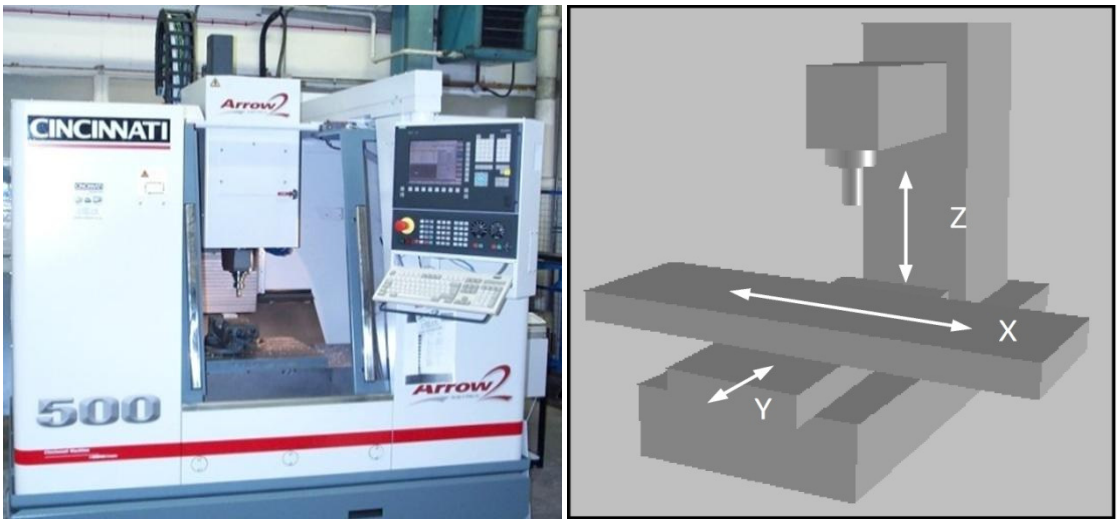

Figure 1. Machine tool configuration

3.2.2 Applied modal parameter extraction technique

STARStruck software [27] was employed for modal parameter estimation from the experimental data using the SDOF, MDOF and globe rational fractional polynomial (GRFP) methods. It also allows interfacing to external FEA software packages to perform structural dynamic modification analysis. From the measured data it develops a 3-D structural representation and determines the frequency, damping and mode shape parameters.

3.2.3 Testing procedure

(a) Widiyarto et al [17] reported on SIMO experimental modal analysis for the machine under review covering the theoretical background for modal parameter extraction; the experimental set up; and the modal analysis technique for a suspended shaker and stinger taking measurements at 156 points on the structure. The data quality was assessed by measuring the coherence across the bandwidth of interest, and should be close to unity to indicate that the measured response is directly attributable to the input forces and is repeatable. The measurements were then performed for 114 points around the structure and Table 1 summarises those modal parameter results for an excitation in the X-axis applied to a dummy cutter through a table mounted shaker and stinger.

The EMA calculates the modal parameters by employing the frequency analysis of the response and excitation force. The theoretical model for the modal parameter extraction is developed in the frequency domain considering the initial conditions (equation 1). Each vector component represents a motion at a particular point in a specific direction characterised by up to six degree of freedom (DOF) motion. This consists of the translational and rotational motions in and about the three orthogonal axes respectively.

$$\mathbf{M}s^2\mathbf{X}(s) - \mathbf{M}s\mathbf{X}(0) - \mathbf{M}\mathbf{X}(0) + \mathbf{C}s\mathbf{X}(s) - \mathbf{C}\mathbf{X}(0) + \mathbf{K}\mathbf{X}(s) = \mathbf{F}(s) \quad (1)$$

Setting the initial conditions to zero:

$$\mathbf{B}(s)\mathbf{X}(s) = \mathbf{F}(s) \quad (2)$$

Where $\mathbf{B}(s)$ is the system matrix:

$$\mathbf{B}(s) = \mathbf{M}s^2 + \mathbf{C}s + K \quad (3)$$

The System matrix is inverted to obtain the Transfer matrix $\mathbf{H}(s)$ and equation (2) rewritten as:

$$\mathbf{X}(s) = \mathbf{H}(s)\mathbf{F}(s) \quad (4)$$

The transfer function elements in the Transfer matrix can be expressed as the ratio of two polynomial functions, which describe the complete dynamic properties between an input and the corresponding response DOF.

STARStruck [27] applies the following equations and an algorithm utilising the global curve fitting rational fraction least squares (RFLS) method, theory covered by Richardson and Ferranti [28] to estimate the modal parameters of the system from the FRF measurements:

Rational Fraction Form:

$$H(s) = \frac{\sum_{k=0}^{m} a_k s^k}{\sum_{k=0}^{n} b_k s^k} \quad (5)$$

Where: $s=j\omega$

Partial Fraction Form:

$$H_k(s) = \sum_{k=0}^{n/2} \left(\frac{r_k}{s - p_k} + \frac{r_k^*}{s - p_k^*} \right) \quad (6)$$

Where: $p_k = -\sigma_k + s_k = k^{th}$ pole; and r_k = residue for k

(b) Further SIMO experimental modal analysis was carried out by exciting the structure in a single direction and measuring the responses in tri-axial directions with three accelerometers mounted on the spindle (see Figure 2)

(c) Different suspended shaker and worktable mounted shaker experimental configurations were explored to determine the benefits and pitfalls of the selected configuration.

(d) The modal parameters extracted from the measured data for different experimental configurations were found to vary indicating the presence of nonlinearity's in the structure and care was taken not to aggravate their influence during the measurement process.

(e) The results showed that the lowest mode shape obtained for all configurations involved the bending of the column and the head in the Y-direction.

(f) The investigation produced several guidelines for performing reliable experimental modal analysis in order to obtain accurate FRF data and maximise the SNR.

(g) Suspended shaker configurations generated improved data by more accurate input force measurement

(h) The measured FRF from the table mounted shaker configuration produced higher SNR because most of the excitation force was delivered into the structure rather than dissipated by the recoiling of the shaker.

3.2.4 Applied Cutting Force Levels

Liu et al [29] in collaboration reported for the same machine: improved cutting force model for peripheral milling; investigation of the cutting force coefficients in ball end milling [30]; and modelling the dynamics of peripheral milling – Prediction and verification of machined surface topography and roughness [31].

3.2.5 Structural dynamic study in three orthogonal directions using a suspended shaker

Three further experiments were performed:

(a) **Suspended shaker with tool tip excitation and no additional table mass (SSTTNM)**

A low inertia TIRAvib type S514 shaker was suspended using a crane with the dummy cutting tool as the driving point. The machine structure was excited in the Y-axis direction to represent one of the cutting force constituent directions. It breaks any force loop linking the machine worktable and the cutting tool which is the case in a worktable mounted shaker configuration. The high mass of the machine structure may force the shaker to recoil if the mass ratio of the shaker to the machine is relatively small, thus reducing the excitation force magnitude. Figure 2 presents this experimental configuration showing the extra masses attached to the shaker to increase the inertia. This technique produced more accurate FRF's (Figure 4) due to the measurement of only the net excitation force entering the machine tool structure and the most suitable arrangement for comparison with the simulated results shown in section 4.

Table 1. Modal parameter results

Mode	Frequency	Damping	Mode Shape Summary
1	21.14 Hz	3.16 %	Dynamic bending of the column in the XZ plane with in-phase headstock and table rocking in the X-axis
2	59.03 Hz	4.20 %	Dynamic bending of the column in the XZ plane with out-of-phase headstock and in-phase table movements in the X-axis
3	64.44 Hz	1.54 %	Dynamic bending of the column in the XZ plane with out-of-phase headstock and in-phase table movements in the X-axis
4	74.96 Hz	2.05 %	Column and headstock bending in the XZ plane, table out of phase movement with relatively big amplitude and headstock bending
5	79.71 Hz	2.77 %	Column and headstock bending, table out of phase movement with relatively big amplitude and bending of headstock
6	119.06 Hz	2.87 %	Rocking of the headstock in the X-axis and slight dynamic bending of the column in the XZ plane
7	127.79 Hz	2.39 %	Small-amplitude dynamic bending of the table and headstock in the XZ and XY planes respectively
8	140.03 Hz	2.24 %	Column and headstock bending and slight bending on table
9	143.42 Hz	3.24 %	Column and headstock bending and slight bending on table with relatively big amplitude
10	165.01 Hz	1.54 %	Twisting of headstock

(b) Suspended shaker with table excitation and no additional table mass (SSTABNM)

The machine structure was excited at a point on the worktable with the Brüel & Kjær shaker Type 4805 or 4811. A stinger was employed to connect the excitation system to the structure via a work-piece secured on a vice. This experimental configuration was selected because the shaker size prevents the selection of the driving point on the worktable. This method assumed that the work-piece and vice stiffness was much higher than that of the structure.

(c) Suspended shaker with table excitation with additional table mass (SSTABM)

This configuration was similar to configuration (b) except that the Microloc clamping system [32] and Kistler cutting force dynamometer [33] were mounted on the machine worktable adding an extra 81 kg mass into the structure. The clamping of the shaker onto the worktable studied the effect of the force transmission path into the structure and enabled one to predict the machine tool dynamic properties during a normal machining process.

Table 2 shows that definite resonant frequencies occur at around 28 Hz and 49 Hz, varying from one configuration to another. The results from configurations (b) and (c) show that there are possibly two closely coupled modes around each of the resonant frequencies. The results from configurations (a) and (c) show that there is a possible third resonant frequency at about 83 Hz. The variation in the driving point produced different modal parameter results and indicated that the machine tool structure nonlinearity's manifests itself by the occurrence of the closely coupled modes which need closer examination to minimise its effect.

Table 2: Summary of results for suspended shaker experiments

Configuration	(a) SSTTNM		(b) SSTABNM		(c) SSTABM	
Mode No.	Frequency (Hz)	Damping (%)	Frequency (Hz)	Damping (%)	Frequency (Hz)	Damping (%)
1	28.28	2.80	21.42	4.59	26.72	2.50
2	52.99	6.16	28.86	2.22	46.39	6.00
3	94.09	2.85	38.86	2.65	70.41	10.43
4	116.69	2.50	49.34	2.39	83.31	6.90

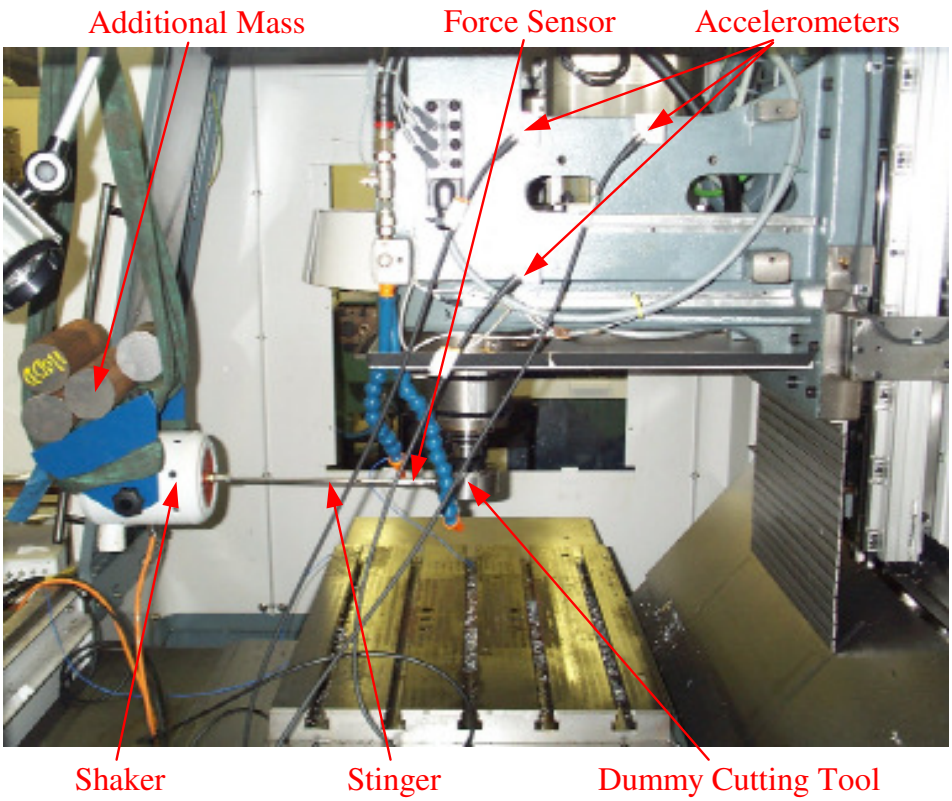

Figure 2: Test layout for tool tip excitation with additional mass

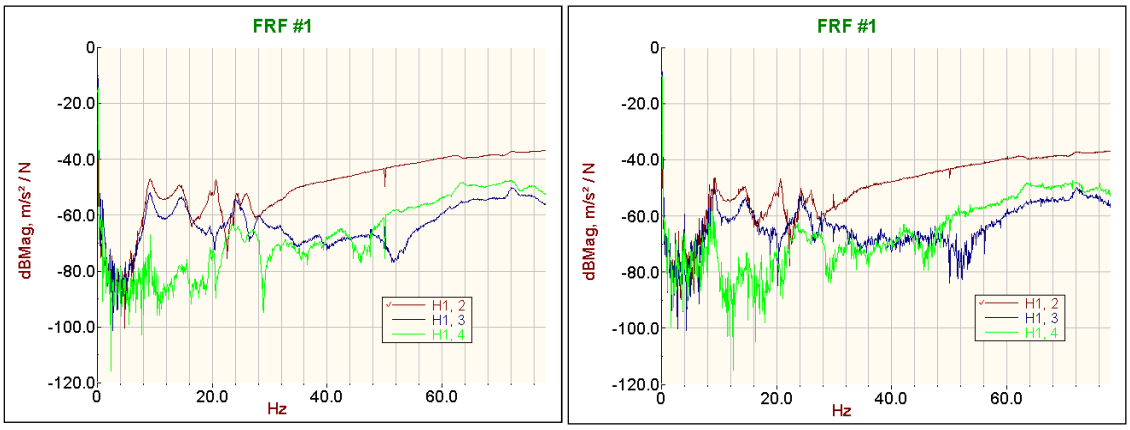

Figure 3: Typical measured FRF's (a) controller off and (b) controller on

3.2.6 Electrical drive consideration

Tests were performed to quantify and determine the effect of energising the control loops during the experiment (Figure 3). No obvious difference in the resonant frequencies and amplitudes between FRF's at the same DOF. The noise content varies between the controller states although there is no clear distinctive pattern. This most probably comes from the electrical circuitry, on considering the results and the fact that headstock position shifts slightly at the instant

where the power to the drives is removed, all experiments in the investigations were performed with the controller switched off.

4.0 Structural dynamic investigation using finite element analysis (FEA)

4.1 Methodology

(a) The FEA model of the machine's structural dynamic properties was developed by closely interfacing a Pro/ENGINEER CAE [34] to a geometrically accurate model of the machine developed by Myers [35]; and utilising an analysis technique reported by Widiyarto [36] to enhance its accuracy. ABAQUS/Standard analysis software [37] and FEMGV [38] were used for FEA pre- and post-processing application to further enhance and improve the machine structural geometry which enabled a more accurate identification of the vibration sources and the modes.

(b) The Pro/ENGINEER physical model was converted for use by ABAQUS/Standard [37] to make use of: improved numerical analysis techniques; software that facilitates parametric studies of the FEA model to be carried out effectively; and a variation in the damping properties of the machine structure, thus enabling a more accurate model to be developed.

(c) Solid modelling software was used to develop the physical model enabling detailed machine geometries such as column and base ribbings to be represented.. The technique also allows non-structural elements with significant mass-effect, such as the Z-axis motor etc., to be modelled relatively easily.

(d) The simulated results were validated against the experimental modal model (section 3); and comparisons made with data from the previous investigations to evaluate the accuracy, processing speed, and geometric requirements.

(e) The validation process also included model updating to improve the discrete model accuracy with respect to the measured dynamic properties by progressively reducing the error. In particular to minimise the deviation between the actual and manufacturer supplied data of the mechanical elements. The summary of the overall procedures undertaken in this structural dynamics study is as shown in Figure 4.

(f) The simulated results were compared to both measured results and simulation data obtained from a reduced FEA model and built-in CAE analysis tools. The measured structural dynamic results were obtained from the EMA using the suspended shaker configuration (section 3).

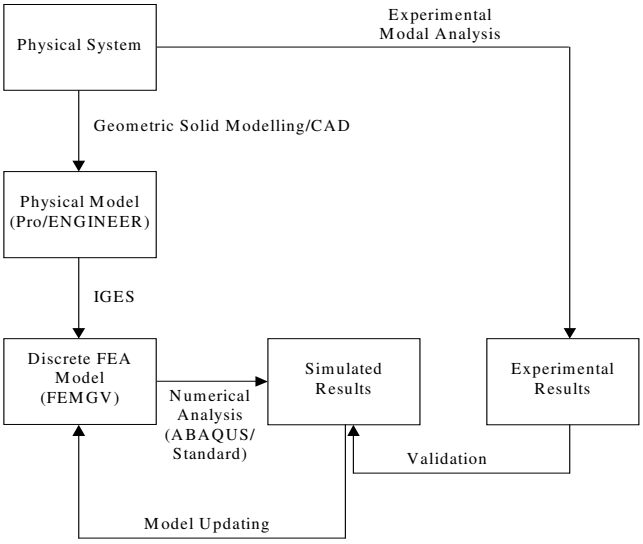

Figure 4: Diagram of the structural dynamic investigation through the FEA and experimental methods

4.2 FEA model development and the numerical analysis using ABAQUS/Standard

The FEA model was produced by the discretisation of the physical model, assignment of material properties to the discrete elements, and definitions of external boundaries and constraints of the system. They were performed in the FEMGEN routine of FEMGV [38] and the result was written to an external file as an input deck to the ABAQUS/Standard package [37]. The complexity of the machine's physical model prevented the use of the quadrilateral and hexahedral elements for the discretisation process as reported by Widiyarto [36] in figure 5b; four node linear tetrahedron (C3D4) continuum elements in Figure 5a were introduced. The Delaunay triangulation technique proposed by Bern et al [39] was utilised to semi-automatically discretise the physical model, involving the manual segment number definitions on the body edges and the automatic mesh generation by the software. The automatic algorithm initially created two-dimensional meshes on surrounding surfaces before three-dimensional mesh containing the tetrahedral elements were formed for the solid model. The algorithm worked by incrementally creating an additional node at the outside of the circumsphere for any tetrahedral in the mesh until all the spatial geometry was completely filled with the elements.

The ratio of the machine element's length and thickness was relatively high which entailed that large numbers of divisions on the longer edges require a large number of finite elements. This was minimised by the use of high performance computing resources and the increased accuracy of the simulation. Nevertheless, an initial investigation was carried out to benchmark the analytical route taken by performing the FEA analysis on the machine base, where mixed element geometries were present but with less complexity (Figure 6).

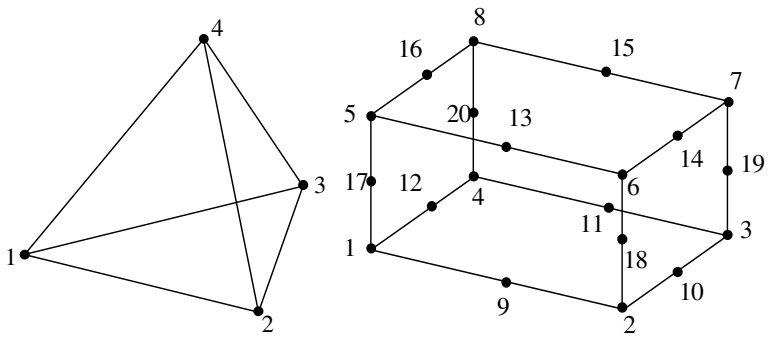

(a) **(b)**

Figure 5 Physical representation of: (a) C3D4 element and (b) C3D20 element

4.2.1 FEA Machine Base

The discretisation of the benchmark physical model produced 126039 tetrahedral elements with 34280 nodes and 102840 variables. The overall quality of the generated finite elements (checked using the standard criteria: minimum angle, aspect ratio, inner-node positioning and radius quotient) was found to be within tolerable limit (97% of the elements satisfied the requirements). The machine base's boundary conditions were defined such that it was considered as rigidly attached to the ground on all of the supporting legs and the base material properties are shown in table 3. An input deck was then generated for the numerical analysis using the ABAQUS/Standard software [37].

The subspace eigensolver method was selected as the numerical method to solve the generated FEA which presented the dynamics of the system as an eigenvalue problem and derived the solution from the linear perturbation of the equilibrium equation:

$$\left(\mu^2\mathbf{M} + \mu\mathbf{C} + \mathbf{K}\right)\boldsymbol{\psi} = 0 \tag{8}$$

The eigenvalues, and thus the natural frequencies, were calculated by assuming that the stiffness matrix was symmetric with negligible damping values. Equation (8) can therefore be represented in a simplified form as:

$$\left(-\omega^2\mathbf{M} + \mathbf{K}\right)\boldsymbol{\psi} = 0 \tag{9}$$

Where:

$$\mu = i\omega \tag{10}$$

Based on these equations, a numerical iteration was carried out to find a solution for a small set of base vectors (a subspace). This solution was subsequently utilised to obtain the structural space containing the lowest eigenvectors which defined the mode shapes. The default dimension of the subspace vectors (m) was defined using equation (4) where p is the number of eigenvectors requested.

$$m = \min(2p,\ p + 8) \tag{11}$$

The numerical analysis was performed on a PC with: a mobile intel core i7 cpu 2.5- 3.4 GHz; parallelism set to 8 cores, 8 Gig Ram (6 Gig set to be used by ABAQUS); and a Windows 7 professional operating system. Utilising the default ABAQUS/Standard version 10 environment configuration, a numerical convergence was obtained in 4 minutes and yielded simulated natural frequencies of 131, 140, 176, 225, and 280 Hz. These frequencies were relatively high compared to the measured results, but considering that less mass was present in the structure and the higher stiffness values, the results were regarded as sufficiently accurate for the given structure.

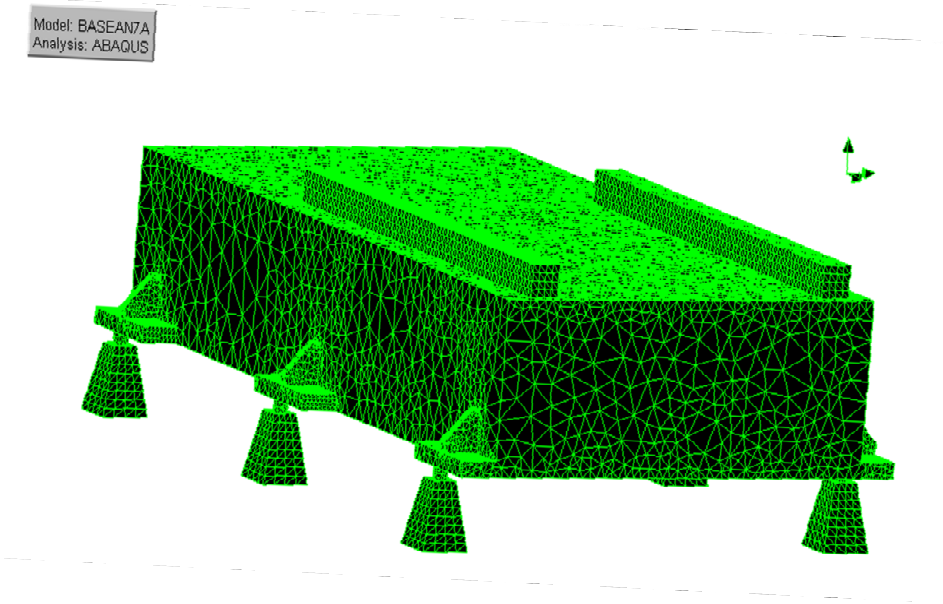

Figure 6: Discrete model for the machine base

4.2.2 FEA machine

An input deck is generated for the full FEA model of the machine and Table 3 lists the material properties for the machine elements. The ball-screws are modelled as beam elements and assumed as shafts in order to calculate the stiffness values. The bearing elements are modelled as spring connectors using the manufacturer-supplied stiffness values.

The boundary conditions for the FEA model are defined as the same as those for the benchmark test. The physical model discretisation using the semi-automatic method generates 469864 tetrahedral elements and 128554 nodes. These elements are also benchmarked against the ideal element criteria (see section 4.2.1), including an additional requirement for the radius ratio, and 96.1 % of them are found to fully satisfy the ideal conditions. Figure 7 shows the colour-coded discretised FEA model for the complete machine structure, illustrating the differing finite element qualities.

The same subspace eigensolver numerical analysis was employed to find the solutions. The analysis was performed using the dedicated PC arrangement (section 4.2.1).The numerical convergence was reached after 20 minutes and the first ten simulated modes can be seen in Table 4. The first mode shape is represented by the column bending motion in the YZ plane. Further analysis of the mode shape shows that the maximum displacement occurs at the spindle motor top (Figure 7). The minimum displacement occurs at the bottom surface of the machine supports/legs where the constraint boundaries are defined. The full results of the mode shape motions are summarised in Table 4.

Table 3. Material properties assigned for the machine tool elements

Machine Element	**Material**	**Young's Modulus** (Nm^{-2})	**Poisson's Ratio**	**Density** (kgm^{-3})
Base (inc. supports)	Cast Iron	1×10^{5}	0.26	7×10^{-9}
Table	Cast Iron	1×10^{5}	0.26	7×10^{-9}
Saddle	Cast Iron	1×10^{5}	0.26	7×10^{-9}
Column	Cast Iron	1×10^{5}	0.26	7×10^{-9}
Spindle Motor	Cast Iron	1×10^{5}	0.26	7×10^{-9}
Spindle Unit	Cast Iron	1×10^{5}	0.26	7×10^{-9}
Cutting Tool	Stainless Steel	2×10^{5}	0.29	7.9×10^{-9}
Ballscrews	Mass less spring	1.95×10^{5}		
X-Axis Bearings	Mass less spring	4.25×10^{5}		
Y-Axis Bearings	Mass less spring	4.91×10^{5}		
Z-Axis Bearings	Mass less spring	5.30×10^{5}		

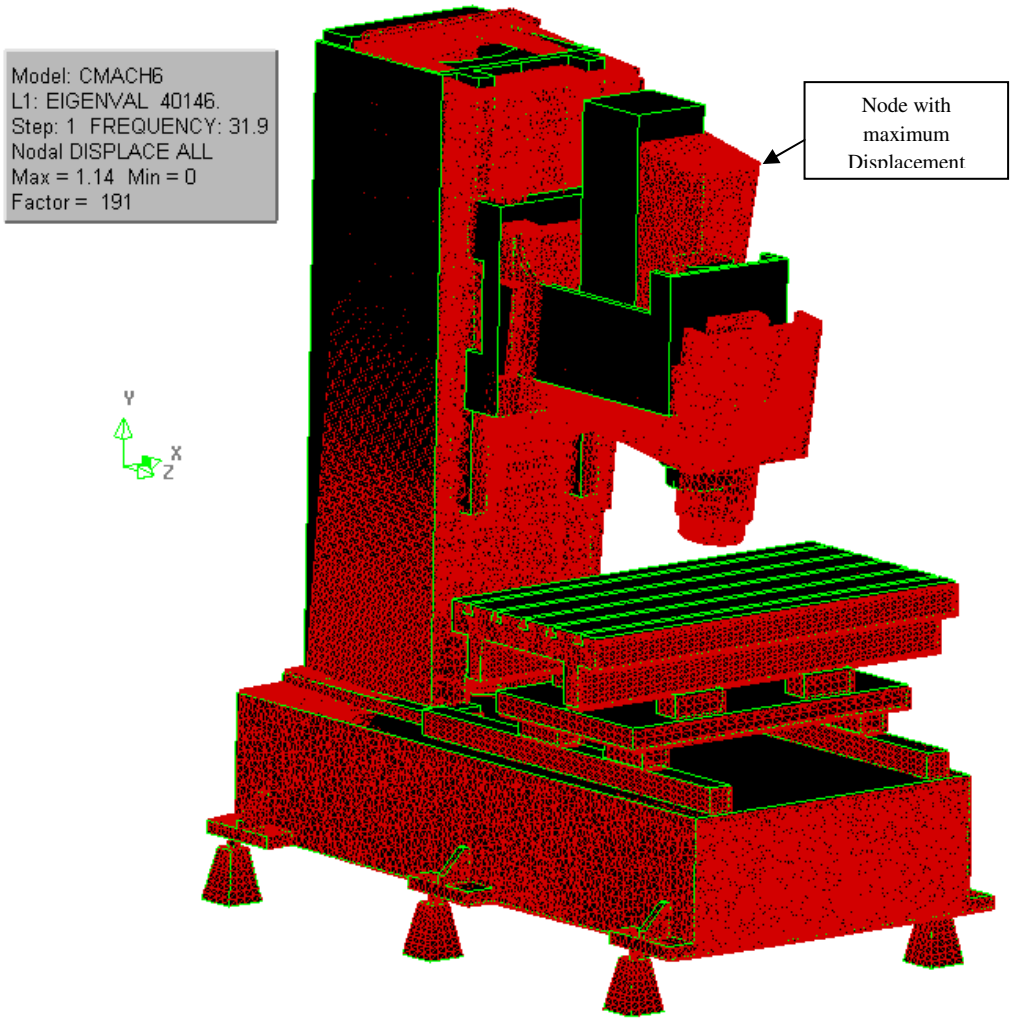

Figure 7: Discrete FEA machine structure model showing mode shape of the first simulated natural frequency (31.87 Hz)

Table 4: The mode shapes of the first ten simulated natural frequencies

Mode	Nat. Freq.	Mode Shape
1	31.87 Hz	Bending motion of column in ZY plane
2	35.80 Hz	Bending motion of column in ZX plane
3	58.18 Hz	Rocking motion of headstock in Z axis and table in ZY plane
4	59.03 Hz	Rocking motion of headstock in Z axis and table rotation about Z axis
5	62.62 Hz	Bending motion of column in ZX plane and rocking of table in Y axis
6	68.93 Hz	Column bending motion in ZY plane, headstock rocking in Z axis, table twisting about Y axis
7	76.20 Hz	Twisting between column and headstock vertically
8	87.48 Hz	Bending motion of column and rocking of spindle motor in ZY plane
9	100.27 Hz	Twisting of headstock in ZY plane caused by rocking of spindle motor
10	108.73 Hz	Twisting of headstock in ZY plane and twisting of table about Y axis

4.3 Comparison with other simulations and experimental results

- For the ABAQUS FEA and Pro/ENGINEER models the numerical convergence time was circa 20 minutes and the FEMGV –ABAQUS model less.
- Table 5 shows the obtained ABAQUS FEA simulation results with respect to the other investigations examined in this study. The results are grouped according to the natural frequency value proximities, showing the percentage differences between outcomes of the previous FEA investigations with respect to the current study. The simulation results in this study contain modes missed by the previous FEA studies. These modes are very likely to be closely coupled, which can only be found due to the larger number of nodes and elements of the FEA model in this study. These modes normally occur in non-linear and axis-symmetric structures, in which the machine structure under study can be categorised.
- The modal parameters extracted for the measured data for different experimental configurations can vary from one another to a small degree. This indicates the presence of structural nonlinearity's and care was taken not to aggravate its influence during the measurement process. The experimental results show that the lowest mode shape obtained in all configurations involves the bending of the column and head in the Y-direction. Thus it can be deduced that the column's structural properties limit the performance of the machine. The investigation has also produced several guidelines for performing reliable EMA in order to obtain accurate FRF data and maximised SNR. The suspended shaker configuration generated the more accurate test and better input force measurement.
- The improved performance of the current ABAQUS model can be clearly seen when you compare Tables 5 and 6. The model produced more modes and natural frequencies some close together. Section 4.2 illustrates the physical model and the need for the assignment of material properties (Table 3). The complexity of the model saw the need for the discretisation process outlined in section 4.2 and shown in Figure 5a. The measurement system has indicated structural nonlinearity's and the material properties required as inputs (e.g Youngs modulus, poisson ratio and density) are nominal values which themselves could be subject to tolerances. The machine boundary conditions are defined such that is considered rigidly attached to the ground on all supporting legs. With sensitivity analysis and more consideration for joints the model could be further improved.
- The simulation results of this study are also compared to those obtained from the experimental technique (Table 6). The simulation results are again grouped with the closest measured natural frequencies. The simulation results reveal some modes which might have been missed during the measurements or the modal parameter extraction process. Several of the likely causes are the limited number of measured points during the

experiment which lower the data resolution and the constrained excitation direction (only in Y-axis) causing only small movement in the perpendicular direction (X-axis). In addition, the detected motion in the perpendicular direction does not produce high coherence values resulting in the rejection of the data during the parameter extraction process.

- The higher values of the simulated natural frequencies when compared to the measured data could be caused by the higher than actual stiffness values in the FEA model. The machine tool base is not infinitely rigid attached to the ground as the model suggests. The machine element connections are not infinitely stiff as suggested by the model. These flexibilities are due to the bolting and welding of the components, which are replaced in the simulation by the total merging of the elements' materials. Also, the lower mass value in the model due to the ball-screw and bearing element representation contributes to a slight increase in the natural frequencies. Lack of actual structural damping could result in slightly higher simulated natural frequencies and the probable exposure of weak and hidden modes.
- Close coupled modes are in evidence in the model and the commercial measurement software algorithms could be further improved using wavelet analysis techniques or similar.

Table 5: Comparison of natural frequencies to nearest integer obtained by different FEA methods

Current ABAQUS Model		**FEMGV–ABAQUS**			**Pro/ENGINEER**		
Mode	**Natural frequency (Hz)**	**Mode**	**Natural frequency (Hz)**	**% Diff**	**Mode**	**Natural frequency (Hz)**	**% Diff**
1	**32**				**1**	**37**	**15.6**
2	**36**	**1**	**35**	**2.8**	**2**	**42**	**16.7**
3	**58**	**2**	**51**	**12**			**12.1**
4	**59**	**3**	**60**	**1.7**			
5	**62**						
6	**69**	**4**	**71**	**2.9**			
7	**76**				**3**	**81**	**6.6**
8	**87**						
9	**100**				**4**	**95**	**5.0**
10	**109**						

Table 6: Comparison of natural frequencies from the simulation and experimental methods

FEA Simulation Natural Frequency Results						EMA Results
Current ABAQUS Model (Hz)	% Difference from EMA results	FEMGV-ABAQUS Model (Hz)	% Difference from EMA results	ProENGINEER model (Hz)	% Difference from EMA results	Natural Frequency (Hz)
31.9	12.7					28.3
35.8		34.5		37.0		
58.2	9.8	50.8	4.2	42.0	20.8	53.0
59.0						
62.6		60.1				
68.9		70.5				
76.2				81.0		
87.5	6.6					94.1
100.3				95.0		
108.7	6.8					116.7

5.0 Conclusions

- SIMO and MIMO experimental modal analysis methods utilised suspended and worktable-supported shaker configurations in order to improve the measured data quality. We recommend that the suspended shaker technique be employed in modal analysis studies as opposed to the shaker on table method normally employed (see section 3.2.5).
- Development of an FEA model for the machine tool structural dynamics using solid design, FEA pre- and post-processing, and FEA analysis software were combined to improve geometric and numerical accuracies. The detailed representation of the machine structural geometry enabled a more accurate identification of the vibration sources and the modes.
- The complexity of the model geometry required that tetrahedral elements were employed for the FEA analysis with a Delaunay triangulation technique to generate the mesh.
- The validation and MAC improvement of the FE model was used against the measured data from the EMA using FEMtools [40] correlation analysis (<12.7%).
- Improvement of the FEA model accuracy through incremental model validation against measured results obtained using SIMO and MIMO experimental modal analyses was undertaken
- The simulated results were compared to both measured results and simulation data obtained from a reduced FEA model and built-in CAE analysis and further compared with those results obtained from the experimental modal analysis. A good agreement was obtained for both the natural frequency and mode shape results.

- The simulated frequency analysis results also showed good correlation with the reduced FEA model but more detailed mode shapes were produced.
- The comparison of the simulated mode shapes with those from the CAE model produced good results but the frequencies were quite different. This is probably due to the less accurate representation of the material behaviour in the CAE software despite the very accurate representation of the machine's geometry and mode shapes. Generally, the correlation results obtained between the higher modes were less accurate indicating that the mass parameters of the models vary considerably.
- Further sensitivity analysis and parametric studies should bring the FEA and EMA closer enabling the implementation and design of passive dampers to improve machine tool performance as indicated by Widiyarto [41].
- Pedrammehr et al [42] utilising a machine model developed in CATIA and modal analysis carried out using a ANSYS workbench for comparison with EMA produced a correlation of less than 8%. It was noticeable that his figures were for natural frequencies greater than 100Hz and in that region our figures were within 7%.
- This paper supports the need for structural improvement which was outlined as a requirement for future machine tools and their application in high performance machining [4]. Prime requirements identified were for improved machine tool structure design; improved FEM models; and efficient passive/active damping techniques. Our FEM models has been demonstrated to be a significant improvement on comparative techniques and with further sensitivity analysis together with improved measurement practices will contribute significantly to knowledge in its investigative application into passive /active development practices.
- Finally a comparison with a different machine of similar size, type and configuration [43] shows a similar range of modal parameter results obtained from a similar vibration measurement procedure. Comparison with Table 1 results are as follows: 21 (20); 59 (54); 64 (64); 75 (79); 80 (90); 119 (112); 128 (127); 140 (132); 143 (133); 165 (169). Thus illustrating a common FEM approach could be adopted for like machine type and configuration provided element size, material etc were machine specific.

Funding

This research was supported by EPSRC with grant numbers: GR/R13401/01 and GR/R1335186/01.

Conflict of interest

None declared.

Acknowledgements

The authors would like to thank the EPSRC for grant support and also the industrial collaborating partners.

References

1. Ford DG. Machining to microns – error avoidance or compensation. Conference Proceedings of LAMADAMAP on Laser Metrology and Machine Performance II; 1995: 41-52.
2. Lui XW, Cheng K, Webb D, Longstaff AP, Widiyarto MH. Improved dynamic cutting force model in peripheral milling, Part II: experimental verification and prediction". Int. J Adv Manuf. Technology; 2004; 24: 794-805.
3. Weck M. Meβtechnische Untersuchung und Beurteilung. Springer Verlag; 1997
4. Lopéz de Lacalle LN, Lamikiz A. - Machine tools for high performance machining, Springer Link, ISBN: 978-1-84800-379-8 (Print), 978-1-84800-380-4 (Online), 2009
5. Engin S, Altinas Y. Mechanics and dynamics of general milling cutters Part 1: helical end mills. International Journal of machine tools and manufacturing; 2001; Vol.41; 15: 2195-2212.
6. Engin S, Altinas Y. Mechanics and dynamics of general milling cutters Part 2: inserted cutters. International Journal of machine tools and manufacturing; 2001; Vol.41; 15: 2213-2231.
7. MAL (Manufacturing Automation Laboratories Inc.) on line, www.maline.com
8. Altintas Y. – Manufacturing Automation – Metal Cutting Mechanics, Machine Tool Vibrations, and CNC Design, Cambridge University Press, Cambridge, (ISBN 0-521-65029-1, 0-521-65973-6), 2000
9. Liu XW, Cheng K, Webb D, Luo XC. – Improved Dynamic Cutting Force Model in Peripheral Milling. Part I: Theoretical Model and Simulation, International Journal of Advanced Manufacturing Technology, Issue 20, 2002, pp. 631 – 638
10. Baek DK, Ko TJ, Kim HS. – A dynamic surface roughness model for face milling, Precision Engineering, vol. 20, Issue 3, May 1997, pp. 171–178
11. Urbikain G, Lôpez de Lacalle LN, Campa FJ, Fernández A, Elias A – Stability prediction in straight turning of a flexible workpiece by collocation method, International Journal of Machine Tools & Manufacture; Vol. 54-55, 2012, pp. 73-71, Elsevier
12. Moradi H, Vossoughi G, Movahhedy MR, Ahmadian MT – Forced vibration analysis of the milling process with structural nonlinearity, internal resonance, tool wear and process damping effects, International Journal of Non-Linear Mechanics;Vol.54, 2013, pp.22-34, Elsevier
13. Pislaru C, Ford DG, Holroyd G. – Hybrid Modelling and Simulation of a CNC Machine Tool Axis Drive, Proceedings of the Institution of Mechanical Engineers (ImechE), Part I, Journals of Systems and Control Engineering, vol. 218 / I2, 2004, pp. 111–120

14. NAFEMS Ltd – National Agency for Finite Element Methods and Standards, Head Office: Beckford Street, Hamilton, Lanarkshire, ML3 0ST, UK
15. Baguley D, Hose DR. - Why Do – Finite Element Analysis, Finite Element and Methods and Standards, NAFEMS Ltd, NEL Glasgow 1994
16. Shewchuk JR, - What is Good Linear Finite Element? Interpolation, Conditioning, Anisotropy, And Quality Measures (Preprint), University of California at Berkeley, December 31st 2002
17. Widiyarto MHN, Ford DG, Pislaru C. - Evaluating the structural dynamics of a vertical milling machine, In Proceedings of LAMADAMAP on Laser Metrology and Machine Performance VI, 2003, pp. 421-430, Edited by Ford DG, WIT Press.
18. Stanbridge AB, Ewins DJ. – Modal Testing Using a Scanning Laser Doppler Vibrometer, Mechanical Systems and Signal processing, Vol. 13, Issue 2, pp 255-270, March 1999
19. Schwarz BJ, Richardson MH. – Experimental Modal Analysis, CSI Reliability Week, Orlando, FL, October 1999
20. Ewins DJ. – Modal Testing, Theory and Practice, 2nd Edition, Baldock Research Studies Press, (ISBN 0-86-380218-4), 2000
21. Døssing O. – Structural Testing. Part II: Modal Analysis and Simulation, Brüel & Kjær Application Note, March 1988
22. IRA Maschinenbau GmbH – Technical Documentation: Vibration System TV51120-M, Schalkau, Germany, 10 December 2001
23. Brüel & Kjær – Product Catalogue: Vibration Exciter System – Types 4805, 4811 and 4815, Naerum, Denmark, June 1996
24. PCB Piezotronics: Force/Torque Division – Model 221B02 ICP® Quartz Force Sensor: Installation and Operating Manual, Depew, New York, USA, August 2000
25. The Modal Shop Inc. – Exciter Stingers 2100 Series, Cincinnati, Ohio, USA, November 1997
26. Dataphysics Corporation – SignalCalc Mobilyzer User Manual, San Jose, California, USA, 2001
27. Spectral Dynamics Inc. – STAR System: Reference Manual, Part Number 3405-0114, Issue A, San Jose, November 1994
28. Richardson MH, Formenti DL. – Global Curve Fitting of Frequency Response Measurements using Rational Fraction Polynomial Method. Proceedings of the 3rd International and Modal Analysis Conference (IMAC), Orlando, FL, November 1982

29. Liu XW, Cheng K, Webb D, Luo XC. – Improved Dynamic Cutting Force Model in Peripheral Milling. Part I: Theoretical Model and Simulation, International Journal of Advanced Manufacturing Technology, Issue 20, 2002, pp. 631 – 638

30. Liu XW, Cheng K, Webb D, Longstaff AP, Widiyarto MHN, Jiang XQ, Ford DG. – Investigation of the Cutting Force Coefficients in Ball-End Milling, Proceedings of LAMDAMAP 2003, Huddersfield, UK, 17 July 2003, (ISBN 1-85312-990-9), pp. 45 – 54

31. Liu XW, Cheng K, Webb D, Longstaff AP, Widiyarto MH. – Improved dynamic cutting force model in peripheral milling. Part II: experimental verification and prediction, International Journal of Advanced Manufacturing Technology, vol. 24, no. 11/12, 2004, pp. 794–805

32. Micron Workholding Ltd – Microloc 75 Series, [on-line], UK, Available: http://www.microloc.com, accessed: 25 June 2004

33. Kistler Instrumente AG – 3-Component Dynamometer F_x, F_y, F_z 9255B, Datasheet DB06.9255Bm, Winterthur, Switzerland, February 1991.

34. Parametric Technology Corporation – Pro/ENGINEER Wildfire, 367 – PRO/E WILDFIRE – BRO – 0204, 2004

35. Myers A, Ford DG, Xu Q. – Finite Element Analysis of the Structural Dynamics of a Vertical Milling Machine, Proceedings of International Conference LAMDAMAP 2003, Huddersfield, 2003, (ISBN 1-85312-990-9), pp. 431 – 440.

36. Widiyarto MHN. – Modelling and Passive Correction Investigation of Vibration Induced Machining Errors on CNC Machine Tools, Chapter 7, pp. 164-181 – Structural Dynamic Investigation using the Finite Element Analysis, PhD Thesis, University of Huddersfield, 2006.

37. Hibbitt, Karlsson and Sorensen, Inc. – Getting Started with ABAQUS/Standard, Pawtucket, USA, 2000.

38. Femsys Limited – FEMGV User Manual for Version 6.4-01, Leicester, UK, March 2003

39. Bern M, Eppstein D, Gilbert JR. – Provably good mesh generation, Proceedings of the 31st Annual Symposium on Foundations of Computer Science, IEEE, 1990, pp. 231–241

40. FEMtools – Solver and platform orientated CAE software program. Dynamic Design Solutions NV, Interleuvenlaan 64, B-3001, Leuven, Belgium

41. Widiyarto MHN. - Modelling and passive correction of vibration induced machining errors on CNC machine tools, Chapter 8, pp. 182- 212 – FEA parametric exercise and vibration control analysis, PhD thesis, University of Huddersfield, 2006.

42. Pedrammehr S, Farrokhi H, Rajab AS, Pakzad S, Mahboubkhah M, Ettefagh MM, Sadeghi MH. – Modal analysis of the milling machine structure through FEM and experimental test, Advanced Materials Research, Vols.383-390(2012) pp.6717-6721, Trans Tech Publications, Switzerland.

43. Ford D.G, Myers A, Haase F, Lockwood S, Longstaff AP. – Active vibration control for a CNC milling machine, Proceedings of the Institution of Mechanical Engineers, Part C: Journal of Mechanical Engineering Science published 4th April 2013. On line version of the article can be found at: http://pic.sagepub.com/content/early/2013/04/04/0954406213484224.